

AuNPs/LDHS Assemblies as Nanoarchitectures: Fabrication, Properties and Specific Application as Photocatalysts

Mihaela BIRSANU¹, Dragos MARDARE¹, Magda PUSCASU¹,
Kiyoshi OKADA² and Gabriela CARJA²

¹Department of Chemical Engineering, Faculty of Chemical Engineering and
Environmental Protection, Technical University *Gh. Asachi* of Iasi,
Bd. Mangeron no.71, Iasi 700554, Romania
e-mail:carja@uaic.ro

²Materials and Structures Laboratory, Tokyo Institute of Technology,
4259 Nagatsuta, Midori, Yokohama, 226-8503, Japan

Abstract. Nanostructured formulations based on nanoparticles of gold supported on zinc-cerium substituted anionic clays (denoted as Au/LDHs) and their derived solid solutions were reported for the investigation of photocatalytic performances in the process of Methylene Blue degradation from aqueous solutions with Vis light. The fabrication of Au/LDHs nano-photocatalysts is simple and cost effective based on the structural “memory effect” of the clay matrix in aqueous solution of AuCl₃. XRD, N₂ adsorption- desorption and UV-Vis analysis were used to investigate the structure, size morphologies characteristics and the photoresponsive properties of the samples. The results presented in our work open new perspectives for fabrication of nano-photoresponsive formulations for degradation of toxic organic pollutants from aqueous solutions.

Key words: gold substituted anionic clay, layered double hydroxides; Methylene blue; photodegradation

1. Introduction

In the last years have been increasing demands for catalysts that can eliminate the polluting materials from the environmental, because the environmental deterioration has become a major obstacle [1]. Photocatalytic degradations of the pollutants represent the most extensive solution for removal of organic dyes and toxic contaminants from wastewater. The degradations of dyes by photocatalytic phenomena, where a semiconductor is activated by light irradiation, can release

harmless products in wastewater [1, 2]. The photodegradation of the dyes from aqueous solution can be performed by oxidizing agents produced by photo – Fenton based reactions under visible light using oxidants such as H_2O_2 , ozone or transitional metals [2]. A wide range of semiconductors, that can take action as sensitizers for light reduced redox process, have been used in photocatalytic reactions type ZnO , SnO_2 , but the most applied was TiO_2 due to high oxidative power, photostability and nontoxicity [3, 4]. The degradation of the dyes under different lights is largely depend on the types of catalysts and composition, light intensity, catalyst loading, solution pH, calcinations temperature [5].

Many investigations were oriented to layered double hydroxides, also known as hydrotalcite like compounds (HTLcs), that can be a great extend as environmental-friendly materials, in incipient or derived form, used as photocatalysts or photocatalyst supports for a variety of anion species or pollutants such as synthetic dyes, pesticides [1, 3, 6, 7].

Nanostructured materials type LDHs are characterized by a lamellar layered structure, which enables specific properties such as redox or acid-base properties, developed surface area, mesoporosity, ion exchange capability. Their layered structure is derived from the isomorphic substitution of a fraction of divalent cations by trivalent cations in a brucite – like lattice ($Mg(OH)_2$) and the positive charge is compensated by the intercalation of anions in the interlayer, with the most common CO_3^{2-} . These materials are a class of synthetic two dimensional nanostructured anionic clays, with favorable textural and acid base properties, as well as anion exchange [1].

The positively charged cationic layers are bound together by the inter-layer anions, as well as hydration water molecules [8, 9]. The majority of anionic clays type layered double hydroxides (LDHs) are described by the general formula $[M(II)_{1-x}M(III)_x(OH)_2^{x+}(A^{n-})_{x/n} \cdot mH_2O]$, where $M(II)$ represents divalent metal ions, $M(III)$ trivalent metal ions, A^{n-} intercalated anions, n is the amount of water in the crystal and x represents the molar ratio of trivalent metal ions to all metal ions, x being the ratio between $M(III)$ and total metal amount $M(III) + M(II)$ [1, 10, 11].

The most attractive features of the nanostructured materials type LDHs is “so-called” structural “memory effect”. Thermal treatment of LDHs leads to the collapse of the layered structure and the formation of highly active metal mixed oxides with high surface area and thermal stability. Based on the manifestation of the LDHs structural “memory effect”, have been reported a simple procedure for obtaining nanoparticles of metal oxides – LDHs ($Me_xO_y/LDHs$) as self-assemblies [12,13]. These calcined layered double hydroxides have the capability to restore the original layered structure by treatment with aqueous solutions containing anions and also to adsorb the metal cations of the aqueous solution [9, 13, 14].

Considering the advantage of characteristic memory effect of LDHs materials, this work has been focused to synthesize new nanostructured photo-responsive catalytic formulations of $ZnCeAILDH$ clay reconstructed in $AuCl_3$ aqueous

solutions and because highly dispersed gold nanoparticles supported on different metal oxides have been demonstrated to be active in many reactions [15]. The obtained materials were characterized by *X-Ray Diffraction (XRD)*, *Transmission Electron Microscopy (TEM)* and *UV-Vis spectroscopy*.

The photocatalytic performances of nanostructured formulations based on gold substituted hydrotalcite type anionic clays supporting on cerium oxides was investigated for the degradation of heterocyclic aromatic chemical compound like *Methylene Blue (MB)* under visible light irradiation.

2. Experimental

2.1. Catalyst Synthesis

The hydrotalcite like clay denoted ZnCeAILDH1 and ZnCeAILDH2 were obtained by coprecipitation method following the procedure described elsewhere [16, 17]. The difference between the samples consists in molar ratio of cerium in the hydrotalcite like clay. Au/ZnCeAILDH1 and Au/ZnCeAILDH2: 1g of “freshly” calcined clays (the anionic clays were calcined at 550°C for 9 h) was added, under vigorous stirring in 150 mL of a 0.1 M aqueous solution of AuCl₃. Cl⁻ was used as an anion source for the structural reconstruction of the clay interlayer. The obtained samples were aged at room temperature for 1h, washed with double deionized water, dried in air and were denoted as Au/ZnCeAILDH1 and Au/ZnCeAILDH2. After calcinations at 600°C for 8h the samples were denoted as Au/ZnCeAILDH1 600 and Au/ZnCeAILDH2 600, respectively.

2.2. Instruments and Techniques

Structural characteristics, cristallinity and purity information were recorded by power *X-Ray Diffraction (XRD)* using a Philips Cubix Pro with Cu K α radiation at 45 kV and 40 mA in the range form 5° to 70°. *Transmission Electron Microscopy (TEM)* observation was performed on the Philips CM 10 transmission electron microscope operating at an accelerating voltage of 100 kV. Also the surface morphology was probed with *field emission scanning electron microscopy FESEM Mira II LMU Tescan*. UV-Vis absorption spectra were recorded on a Jasco V 550 spectrophotometer with integration sphere. Elemental analysis was performed by ICP emission spectroscopy using solution prepared by dissolving the samples in dilute H₂SO₄. Specific surface areas (S_{BET}) were determined using the Brunauer Emmett Teller method based on adsorption-desorption [13, 18].

2.3. Photocatalytic Activity Measurement

Photocatalytic activity for all the samples was tested by degradation of dye molecules of *Methylene Blue (MB)*. Photocatalysis study was carried out by using

25 mg of catalyst in 25 mL of solution containing *Methylene Blue* (MB) with an initial concentration of dyes equal to 40 mg/L. Prior to the catalytic experiments the aqueous solution with the dye and the catalyst were stirred in the dark for about 1h to establish the adsorption–desorption equilibrium, until the dye concentration remained constant. The weight of the catalyst was always maintained the same (1g/L). A 200 W xenon doped mercury lamp (Hamamatsu Lightningcure LC8), with a cutoff filter for visible light irradiation ($\lambda > 420$ nm) was used as the light source for the photocatalytic reaction. The degradation of MB was conducted also using oxidizing agents in form of H₂O₂ with MB: H₂O₂ molar ratio of 1:1, 1:2 and 1:5. All the photocatalytic experiments were performed at room temperature. During the irradiation, at different time intervals, samples of the suspension were collected, centrifuged to remove the catalyst and then monitored by UV–Vis analysis following the intensity of the absorption peak at a wavelength 664 nm characteristic MB. The blank reaction was doing following the same procedure without the catalyst.

3. Results and Discussion

3.1. Characterization of the Photocatalysts

The result of the quantitative analysis, carried out by ICP emission spectroscopy, surface areas and pore volume of the materials are presented in Table 1. The decrease of the surface area and the pore volume for the mixed oxides obtained from the reconstructed clays can suppose less emphasized porous property for clays matrices. The crystalline structure of the studied samples, in their as-synthesized form and after reconstruction process in AuCl₃ solution was characterized by XRD.

Table 1. Various physical-chemical properties of the catalysts

Sample	ICP Au Atomic ratio (%)	S _{BET} (m ² /g)	V _p (cm ³ /g)
Au/ZnCeAILDH1	4.98	57	0.349
Au/ZnCeAILDH1 600	4.94	19	0.210
Au/ZnCeAILDH2	4.79	54	0.387
Au/ZnCeAILDH2 600	4.78	32	0.348

Figure 1A and B illustrates the power *X-Ray Diffraction* of the LDH like clays and the *X-Ray Diffraction* pattern for the calcined samples. It reveals the presence of a single crystalline phase with the reflections assigned to the layered structure, with sharp and symmetric basal reflection of (003), (006) and (009) planes, at low 2θ angles and broad, less intensive and asymmetric reflections for the non-basal (012), (015) and (018) planes, at high 2θ angle [19, 20]. Low intensity peaks, also observed, can be assigned to the presence of crystalline ZnO phase dispersed over the brucite like layers and also a second phase of cerium oxide, indicating that

cerium ions are not only in the lamellar structure [4, 21]. Calcination of the samples leads to the collapse of the layered structure and new diffraction peaks appear.

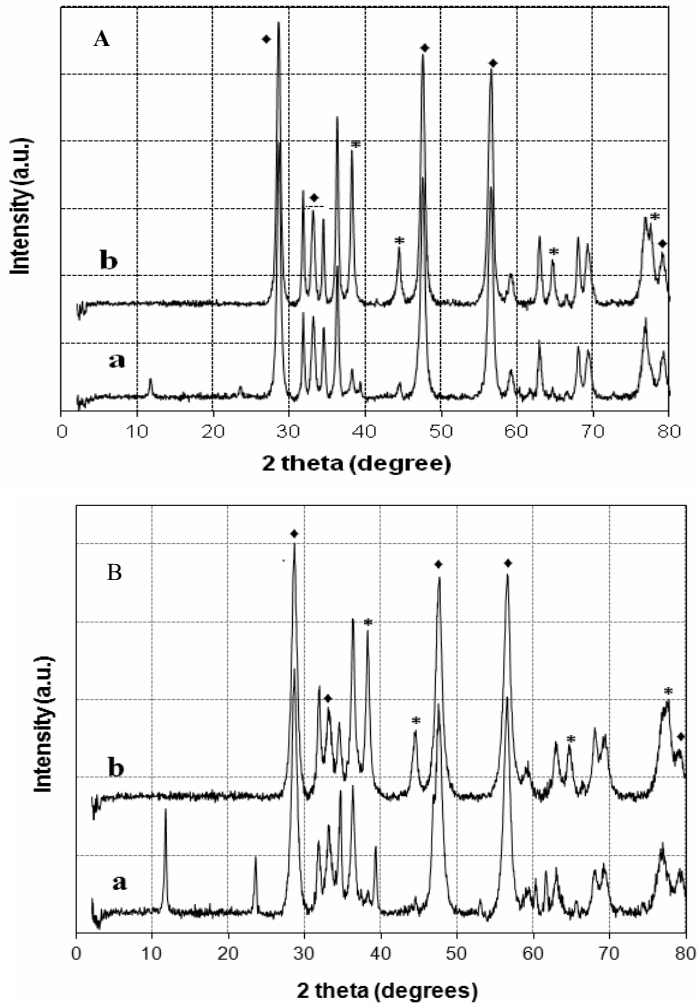


Fig. 1A. XRD patterns for Au/ZnCeAlLDH1 (a) reconstructed clay and (b) calcined clay at 600°C; **B.** XRD patterns for Au/ZnCeAlLDH2 (a) reconstructed clay and (b) calcined clay at 600°C; (◆) CeO₂; (*) Au.

The XRD diffractograms of the calcined samples reveals the decomposition of the LDHs phase leading to zincite ZnO (wurtzite JCPDS file No. 36-1451) phase and the spinel phase ZnAl₂O₄ (JCPDS file No. 5-0669) [13] and face centered cubic structure of CeO₂ with narrow two theta signals at 28.6°, 33.1°, 47.5°, 56.5° and 79.1°, which could be indexed to the (111), (200), (220), (311), (331) [15].

Samples, typically violet-colored as expected for the gold deposited on LDHs, exhibits a surface plasmon band with the intensity proportional with gold particles size [26]. Also, the spectra show the existence of gold in the prepared nanoparticles system. The diffraction peaks at 2θ : 38.4° , 44.6° , 64.8° and 77.8° were indexed to the crystal planes (111), (200), (220), (311) of gold cubic phase (JCPDS Card No. 65-2870) [22].

In photocatalytic activity, important information about the photoresponsive properties of the materials can be supplied by the optical spectrum. The optical absorption of reconstructed samples and derived mixed oxides in the UV–Vis region is shown in Fig. 2.

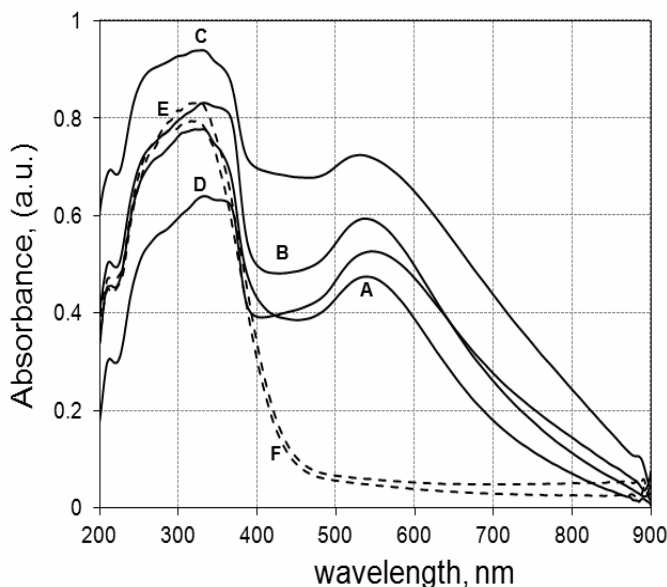


Fig. 2. UV-Vis absorption spectra of: (A) Au/ZnCeAlLDH1; (B) Au/ZnCeAlLDH2; (C) Au/ZnCeAlLDH1 600; (D) Au/ZnCeAlLDH2 600; (E) ZnCeAlLDH1; (F) ZnCeAlLDH2.

The addition of gold nanoparticles introduces a new band in the visible region around 550 nm attributed to the surface plasmon resonance [23, 24], absorption that is realized by the collective oscillation of the conduction band electron of gold nanoparticles as response to the optical excitation [25].

The XRD and UV–Vis results point out the formation of the nanoparticles of gold deposited on ZnCeAlLDH clay matrices and that the calcinations process transforms the hydrotalcite like anionic clays into $\text{CeO}_2/\text{ZnO}/\text{ZnAl}_2\text{O}_4$ phase with the increase of the gold nanoparticles size of dispersed on the larger nanoparticles of LDHs.

3.2. Photocatalytic Activity

The photocatalytic activity of as-synthesized and calcined samples was evaluated using the photocatalytic degradation of the aqueous solutions of the Methylene Blue dye under visible light. Temporal evolution of the spectral changes during the photodegradation of MB using is shown in Fig. 3A while the photocatalytic efficiency of the catalysts is presented in Fig. 3B. The derived solid solutions displayed lower photocatalytic efficiency, thus the removal efficiency of MB apparently decrease by almost 6% for the calcined samples over the entire range of wavelength. For the parent clay ZnCeAILDH1 and ZnCeAILDH2, the MB degradation efficiency is 10% and 16% respectively.

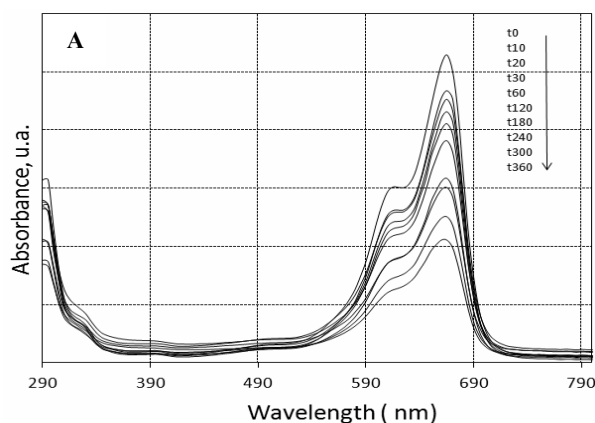


Fig. 3A. Temporal evolution of the UV Vis spectral changes taking place during the photodegradation of MB on Au/ZnCeAILDH2 600.

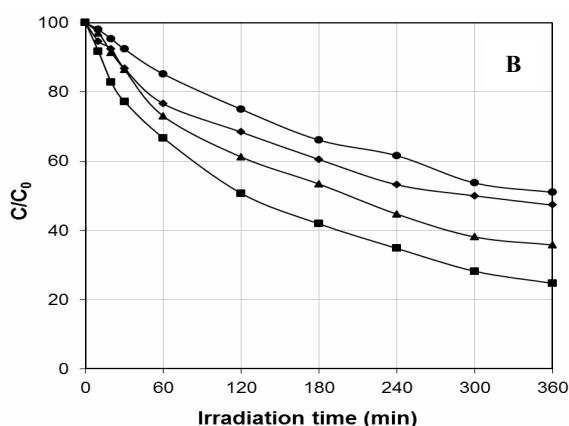


Fig. 3B. Comparison of the photocatalytic efficiency of the catalysts during the photodegradation process of MB over the entire range of wavelength; ● Au/ZnCeAILDH1 600; ◆ Au/ZnCeAILDH1; ▲ Au/ZnCeAILDH2; ■ Au/ZnCeAILDH2 600.

The experiments were carried out in presence of visible light also using an oxidizing agent H_2O_2 thus providing that the dye is decolorized by photo Fenton reaction. Figure 4A shows the temporal evolution of the spectral changes and Fig. 4B presents comparison of the rate of degradation of MB dye in presence of visible light and Au/ZnCeAILDH2 catalyst using different molar ratios of hydrogen peroxide and MB. Hydrogen peroxide concentration is an important parameter for the degradation of the dye in heterogeneous photo- Fenton reaction. H_2O_2 was decomposed at the surface of catalyst to generate hydroxyl radicals. The increase of hydrogen peroxide concentration would lead to more hydroxyl radicals produced.

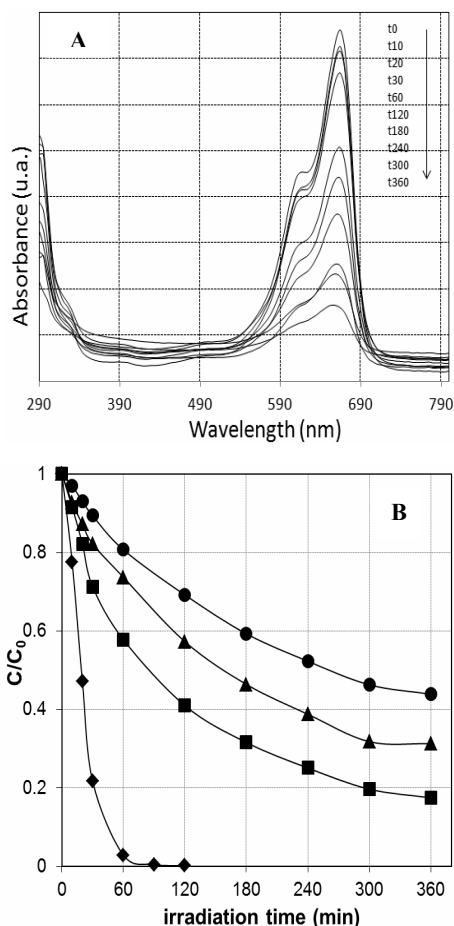


Fig. 4A. Temporal evolution of the UV Vis spectral changes taking place during the photodegradation of MB on Au/ZnCeAILDH2 600 using H_2O_2 ; **B.** Comparison of the photocatalytic efficiency of the catalysts during the photodegradation process of MB over the entire range of wavelength using different molar ratios MB: H_2O_2 ;
 ● without H_2O_2 ; ▲ 1 mol H_2O_2 ; ■ 2 moles H_2O_2 ; ◆ 5 moles H_2O_2 .

At low concentration, H_2O_2 could not generate enough hydroxyl radicals and the degradation efficiency was slow. It can be observed that using a lower concentration of hydrogen peroxides the degradation of the dye reached nearly 70% for 1M of H_2O_2 and 82% for 2M of H_2O_2 respectively, after 6h of irradiation. If we increase the amount of hydrogen peroxide at 5 M, the degradation of the dye solution is completely after 3h of irradiation with visible light; however the decolorization of Methylene blue increased significantly with the increase of amount of hydrogen peroxide. This is because the hydroperoxyl radicals ($\bullet\text{HO}_2$) are produced in presence of a local excess of H_2O_2 [27]. The degradation of MB dye likewise under the same conditions was studied by using the dye solution without the catalysts as reference sample. It was found that any degradation of the dye take place during the photodegradation process using visible light irradiation.

4. Conclusions

The results of the present work show the successful synthesis nanoparticles of gold deposited on the layered matrix of the anionic clays by using the structural reconstruction of the ZnCeAILDH clays in AuCl_3 aqueous solutions. The calcinations process converts anionic clays type LDHs into mixture of mixed oxides and increase the size of gold nanoparticles. The morphology and structure of nanostructured materials have been analyzed by various methods. These nanostructured assemblies, especially Au/ZnCeAILDH2, showed an efficient photodegradation of the dye Methylene Blue under visible light irradiation. Also it was found that the samples had a highly catalytic activity for degradation of MB in presence of H_2O_2 and visible light. The new nanostructures Au/LDHs may contribute to open new perspective for the facile fabrication of cheap nano-photoresponsive formulations for removal of toxic pollutants from wastewater.

Acknowledgements. This work was supported by the grant of the Romanian National Authority for Scientific Research, CNCS-UEFISCDI, Project number PN-II-ID-PCE-75/2013.

References

- [1] M.S. HADNADEV-KOSTIC, T.J. VULIC, D.B. ZORIC, R.P. MARINKOVIC-NEDUCIN, *Chem. Ind. Chem. Eng. Q.* **18**, pp. 295–303, 2012.
- [2] T. WARANG, N. PATEL, R. FERNANDEZ, N. BAZZANELLA, A. MIOTELLO, *Appl. Catal. B* **132-133**, pp. 204–211, 2013.
- [3] X. LIU, X. ZHAO, Y. ZHU, F. ZHANG, *Appl. Catal. B* **140-141**, 241–248, 2013.
- [4] M. HADNADJEV-KOSTIC, T. VULIC, J. RANOGAJEC, R. MARINKOVIC-NEDUCIN, A. RADOSAVLJEVIC-MIHAILOVIC, *J. Therm. Anal. Calorim.* **111**, pp. 1155–1162, 2013.
- [5] S. SHAKTIVEL, B. NEPPOLIAN, M.V. SHANKAR, B. ARABINDO, M. PALANICHAMY, V. MURUGESAN, *Sol. Energ. Mat. Sol.* **C77**, pp. 65–82, 2003.
- [6] F. ZHANG, X. XIANG, F. LI, X. DUAN, *Catal. Surv. Asia* **12**, pp. 253–265, 2008.

- [7] D.G. EVANS, R.C.T. SLADE, *Structure Bonding*, pp. 1191–1287, 2006.
- [8] P. BENITO, J. LABAJOS, J. ROCHA, V. RIVES, *Microporous Mesoporous Mat.* **94**, pp. 148–158, 2006.
- [9] G. CARJA, Y. KAMESHIMA, A. NAKAJIMA, K. OKADA, *Mesoporous Mat., Mesoporous Materials: Properties, preparation and applications* **9**, pp. 191–202, 2009.
- [10] A. MANTILLA, F. TZOMPANTZI, J.L. FERNANDEZ, J.A.I. DIAZ GONGORA, R. GOMEZ, *Catal Today*. **150**, pp. 353–357, 2010.
- [11] Z.P. XU, J. ZHANG, M.O. ADEBAJO, H. ZHANG, C. ZHOU, *Appl. Clay Sci.* **53**, pp. 139–150, 2011.
- [12] G. CARJA, A. NAKAJIMA, S. DRANCA, C. DRANCA, K.J. OKADA, *Phys. Chem. C* **114**, pp. 14722–14728, 2010.
- [13] G. CARJA, L. DARTU, K. OKADA, E. FORTUNATO, *Chem. Eng. J.* **222**, pp. 60–66, 2013.
- [14] S. YUAN, Y. LI, Q. ZHANG, H. WANG, *Colloids Surf. A Physicochem. Eng. Asp.* **348**, pp. 76–81, 2009.
- [15] E. SMOLENTSEVA, A. SIMAKOV, S. BELOSHAPKIN, M. ESTRADA, E. VARGAS, V. SOBOLEV, R. KENZHIN, S. FUENTES, *Appl. Catal.* **B115-116**, pp. 117–128, 2012.
- [16] G. CARJA, E. HUSANU, C. GHERASIM, H. IOVU, *Appl. Catal.* **B 107**, pp. 253–259, 2011.
- [17] W.T. REICHLER, S.Y. KANG, D.S. EVERHARDT, *J. Catal.* **101**, pp. 352–359, 1986.
- [18] V. PREVOT, V. BRIOIS, J. CELLIER, C. FORANO, F. LEROUX, *J. Phys. Chem.* **69**, pp. 1091–1094, 2008.
- [19] F. CAVANI, F. TRIFIRO, A. VACCARI, *Catal. Today* **11**, pp. 173–301, 1991.
- [20] Y. KAMESHIMA, H. SASAKI, T. ISOBE, A. NAKAJIMA, K. OKADA, *Int. J. Pharm.* **381**, pp. 34–39, 2009.
- [21] C. GOMES SILVA, R. JUÁREZ, T. MARINO, R. MOLINARI, H. GARCÍA, *J. Am. Chem. Soc.* **133**, pp. 595–602, 2011.
- [22] E. NALBANT ESENTURK, A.R. HIGHT WALKER, *J. Nanopart. Res.* **15**, pp. 1364–1373, 2013.
- [23] I.M. ARABATZIS, T. STERGIOPOULOS, D. ANDREEVA, S. KITOVA, S.G. NEOPHYTIDES, P. FALARAS, *J. Catal.*, **220**, pp. 127–135, 2003.
- [24] J. MATOS, T. MARINO, R. MOLINARI, H. GARCIA, *Appl. Catal.* **A417-418**, pp. 262–272, 2012.
- [25] P.V. KAMAT, *J. Phys. Chem* **B106**, pp. 7729–7744, 2002.
- [26] T. MARINO, R. MOLINARI, H. GARCIA, *Catal. Today* **206**, pp. 40–45, 2013.
- [27] F. JI, C. LI, J. ZHANG, L. DENG, *J. of Hazard. Mater.* **186**, pp. 1979–1984, 2011.